



Supporting Information

Identification of Favorable Silica Surface Sites for Single-Molecule Magnets

Moritz Bernhardt, Lukas Lätsch, Boris Le Guennic,* and Christophe Copéret*© 2023 The Authors. Helvetica Chimica Acta published by Wiley-VHCA AG. This is an open access article under the terms of the Creative Commons Attribution Non-Commercial License, which permits use, distribution and reproduction in any medium, provided the original work is properly cited and is not used for commercial purposes.

Table S1: Average bond distances for the anionic and neutral ligand for all ten investigated model structures.

Model	Averaged bond distance anionic ligands [Å]	Averaged bond distance neutral ligands [Å]
1	2.066	—
2	2.063	—
3	2.142	—
4	2.142	2.153
5	2.142	2.142
6	2.108	2.523
7	2.142	2.177
8	2.122	2.151
9	2.122	2.224
10	2.120	2.688

Table S2: Calculated shielding and the resulting chemical shift for all ten investigated model structures. The experimental spectrum shows a broad signal spanning the range from around -50 to 240 ppm representing a distribution of sites without resolving different species.^[1]

Model	Shielding	Chemical shift [ppm]
1	2715	140
2	2764	104
3	2806	73
4	2711	143
5	2634	198
6	2702	149
7	2705	147
8	2715	140
9	2664	176
10	2708	144

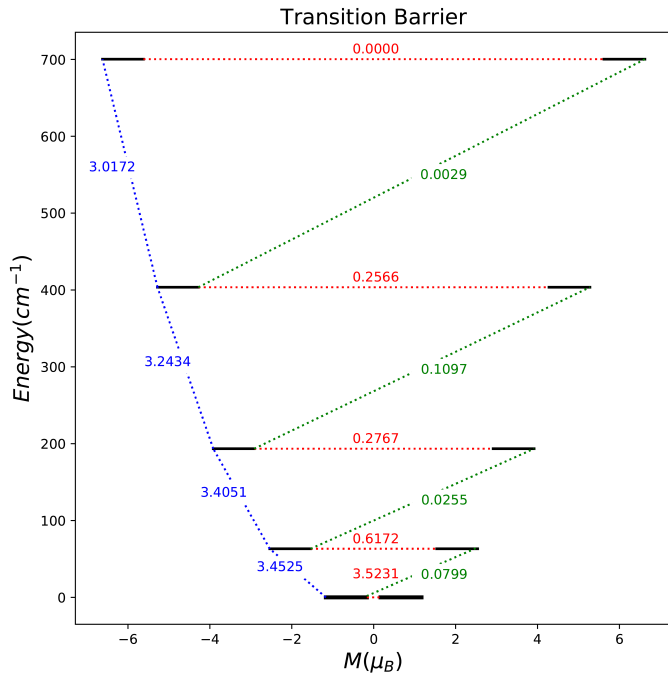


Figure S1: Computed magnetization blocking barriers for **1**. The four lowest Kramers doublets (thick black lines) are represented according to their magnetic moment along the main magnetic axis. The blue lines represent vertical excitations, the green dashed lines correspond to possible Orbach relaxation processes while the red lines correspond to QTM/TA-QTM processes. The values correspond to the mean value of the corresponding transversal matrix element of the transition magnetic moment.

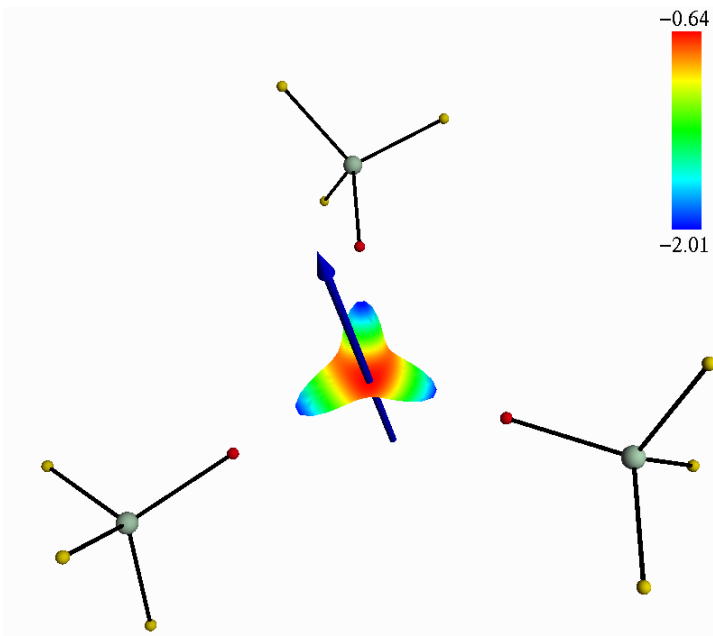


Figure S2: Representation of the total electrostatic potential (expressed in $e^- \cdot \text{bohr}^{-1}$) at 2.5 Å around the Dy(III) ion with g_z direction in blue line for **1**. The lowest and highest values are in blue and red, respectively.

Table S3: Computed energy levels (the ground state is set at zero), composition of the g-tensor and contributions to the wave function for each M_J state of the ground-state multiplet for the model **1**. KD stands for Kramers doublet.

KD	E (cm^{-1})	g_x	g_y	g_z	wave function composition*
1	0	12.406	8.733	1.335	$99.2 \pm 1/2\rangle$
2	63.3	1.515	2.160	4.076	$99.2 \pm 3/2\rangle$
3	193.5	0.487	1.071	6.834	$99.8 \pm 5/2\rangle$
4	403.6	0.761	0.779	9.559	$99.8 \pm 7/2\rangle$
5	700.4	0.012	0.013	12.243	$100.0 \pm 9/2\rangle$
6	1075.5	0.001	0.002	14.799	$100.0 \pm 11/2\rangle$
7	1458.8	0.002	0.002	17.271	$100.0 \pm 13/2\rangle$
8	1693.3	0.000	0.000	19.842	$100.0 \pm 15/2\rangle$

* Contributions $< 10\%$ are omitted.

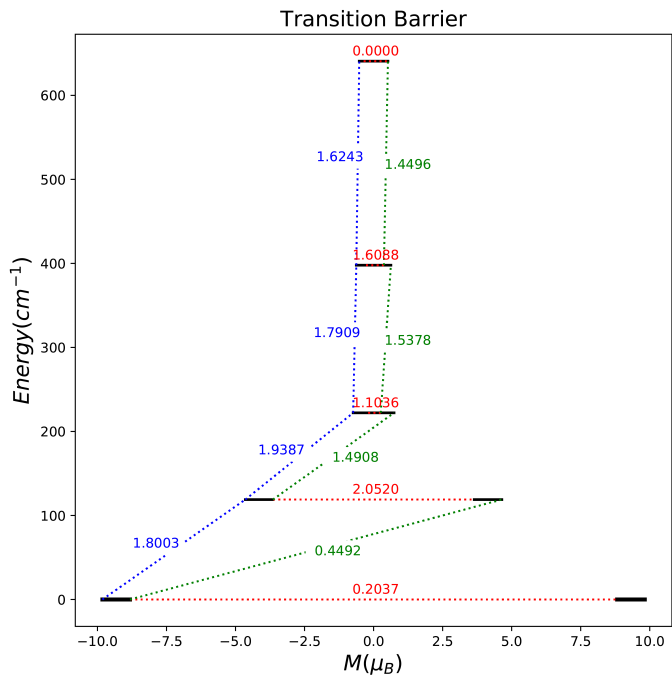


Figure S3: Computed magnetization blocking barriers for **2**. The four lowest Kramers doublets (thick black lines) are represented according to their magnetic moment along the main magnetic axis. The blue lines represent vertical excitations, the green dashed lines correspond to possible Orbach relaxation processes while the red lines correspond to QTM/TA-QTM processes. The values correspond to the mean value of the corresponding transversal matrix element of the transition magnetic moment.

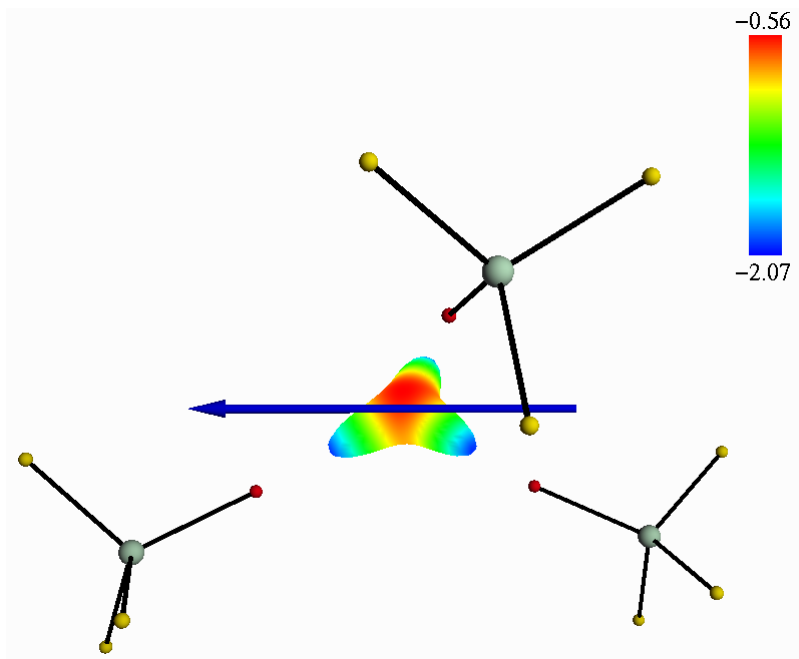


Figure S4: Representation of the total electrostatic potential (expressed in $e^- \cdot \text{bohr}^{-1}$) at 2.5 Å around the Dy(III) ion with g_z direction in blue line for **2**. The lowest and highest values are in blue and red, respectively.

Table S4: Computed energy levels (the ground state is set at zero), composition of the g-tensor and contributions to the wave function for each M_J state of the ground-state multiplet for the model **2**. KD stands for Kramers doublet.

KD	E (cm $^{-1}$)	g_x	g_y	g_z	wave function composition*
1	0	0.314	0.908	18.642	$84.9 \pm 15/2> + 10.7 \pm 11/2>$
2	118.9	9.444	8.288	2.841	$33.2 \pm 13/2> + 23.4 \pm 9/2> + 16.5 \pm 5/2> + 11.7 \pm 1/2>$
3	222.1	0.005	0.481	6.589	$28.5 \pm 13/2> + 21.8 \pm 7/2> + 17.3 \pm 3/2> + 13.4 \pm 11/2>$
4	397.8	0.175	0.253	9.473	$27.4 \pm 11/2> + 22.7 \pm 13/2> + 19.6 \pm 5/2> + 13.6 \pm 1/2>$
5	640.7	0.039	0.059	12.149	$27.8 \pm 11/2> + 23.7 \pm 9/2> + 20.9 \pm 3/2> + 11.0 \pm 13/2>$
6	940.2	0.006	0.010	14.662	$28.7 \pm 9/2> + 25.6 \pm 7/2> + 18.8 \pm 1/2> + 14.8 \pm 11/2>$
7	1249.4	0.003	0.003	17.187	$31.7 \pm 5/2> + 26.8 \pm 7/2> + 19.6 \pm 3/2> + 13.6 \pm 9/2>$
8	1507.9	0.000	0.000	19.756	$39.9 \pm 1/2> + 30.7 \pm 3/2> + 17.9 \pm 5/2>$

* Contributions < 10% are omitted.

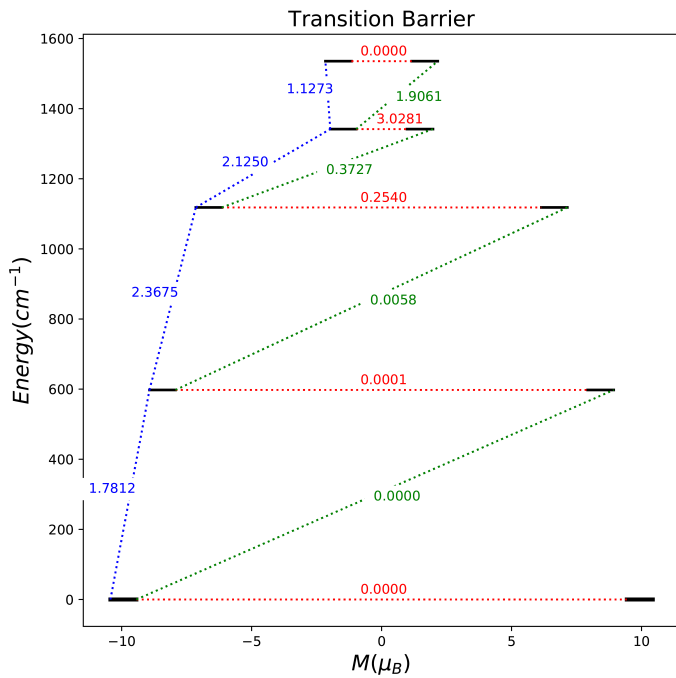


Figure S5: Computed magnetization blocking barriers for **3**. The four lowest Kramers doublets (thick black lines) are represented according to their magnetic moment along the main magnetic axis. The blue lines represent vertical excitations, the green dashed lines correspond to possible Orbach relaxation processes while the red lines correspond to QTM/TA-QTM processes. The values correspond to the mean value of the corresponding transversal matrix element of the transition magnetic moment.

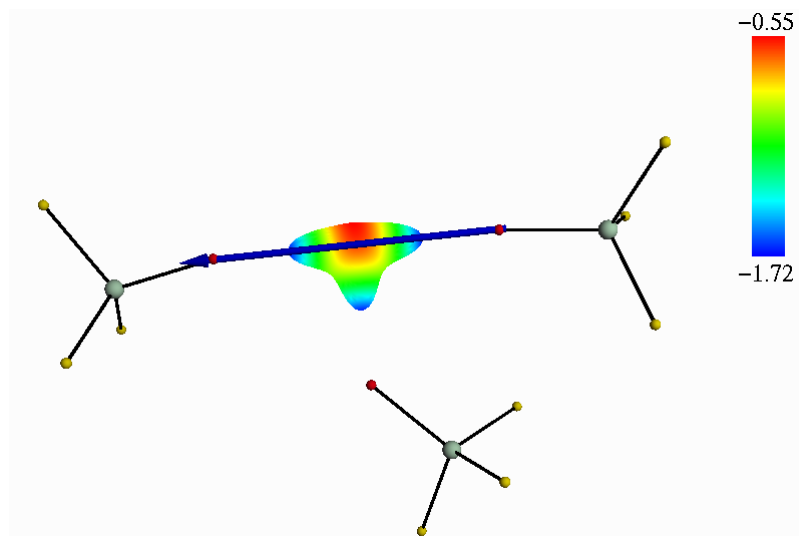


Figure S6: Representation of the total electrostatic potential (expressed in $e^- \cdot \text{bohr}^{-1}$) at 2.5 Å around the Dy(III) ion with g_z direction in blue line for **3**. The lowest and highest values are in blue and red, respectively.

Table S5: Computed energy levels (the ground state is set at zero), composition of the g-tensor and contributions to the wave function for each M_J state of the ground-state multiplet for the model **3**. KD stands for Kramers doublet.

KD	E (cm ⁻¹)	g_x	g_y	g_z	wave function composition*
1	0	0.000	0.000	19.867	$99.9 \pm 15/2>$
2	597.6	0.000	0.000	16.858	$98.8 \pm 13/2>$
3	1118.3	0.535	0.988	13.296	$88.4 \pm 11/2>$
4	1341.6	2.949	4.186	13.995	$31.6 \pm 1/2> + 24.2 \pm 5/2> + 20.3 \pm 9/2> + 16.5 \pm 3/2>$
5	1535.4	3.305	3.610	9.711	$47.9 \pm 9/2> + 23.8 \pm 3/2> + 13.4 \pm 7/2>$
6	1808.7	0.395	1.155	13.805	$38.3 \pm 7/2> + 21.8 \pm 9/2> + 20.8 \pm 1/2> + 12.5 \pm 5/2>$
7	2112.1	0.247	0.389	16.889	$37.5 \pm 5/2> + 29.6 \pm 7/2> + 21.4 \pm 3/2>$
8	2317.4	0.007	0.025	19.712	$38.5 \pm 1/2> + 32.0 \pm 3/2> + 20.3 \pm 5/2>$

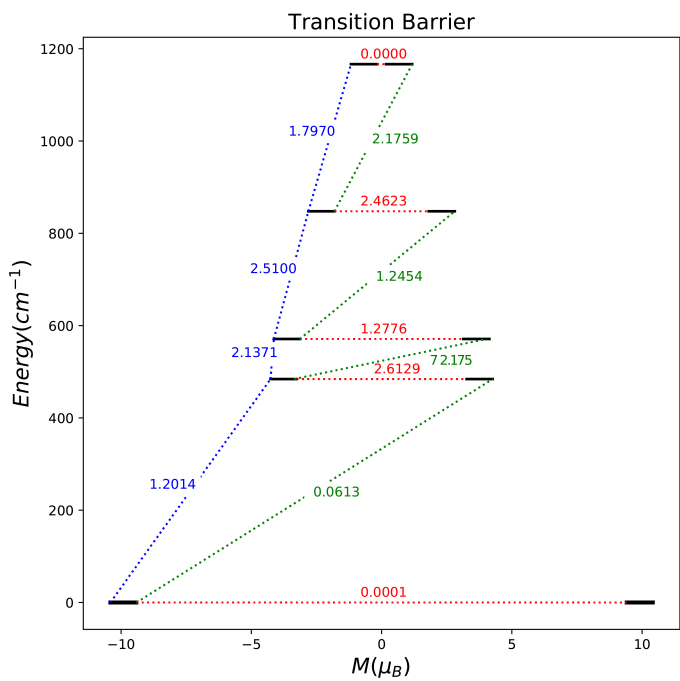


Figure S7: Computed magnetization blocking barriers for **4**. The four lowest Kramers doublets (thick black lines) are represented according to their magnetic moment along the main magnetic axis. The blue lines represent vertical excitations, the green dashed lines correspond to possible Orbach relaxation processes while the red lines correspond to QTM/TA-QTM processes. The values correspond to the mean value of the corresponding transversal matrix element of the transition magnetic moment.

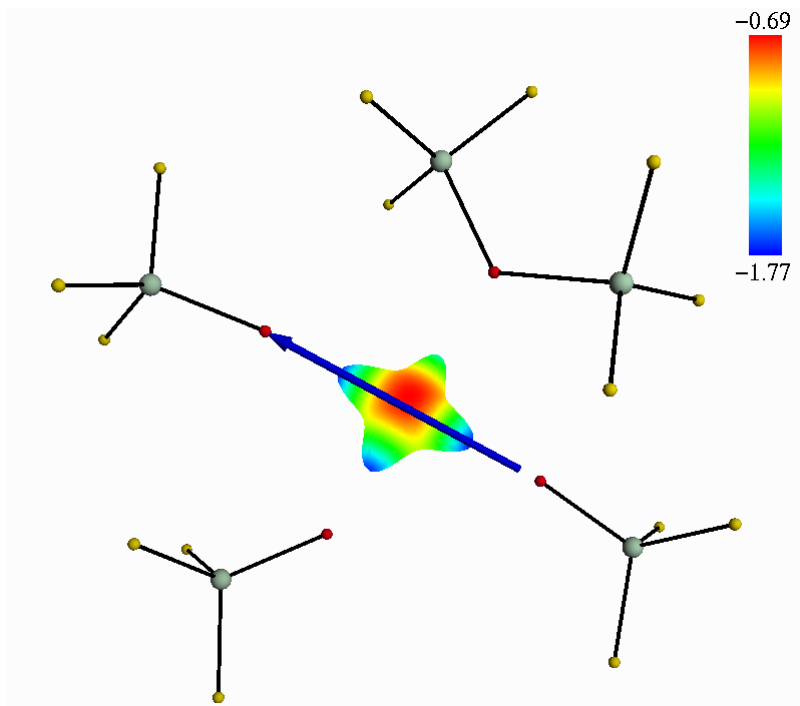


Figure S8: Representation of the total electrostatic potential (expressed in $e^- \cdot \text{bohr}^{-1}$) at 2.5 Å around the Dy(III) ion with g_z direction in blue line for **4**. The lowest and highest values are in blue and red, respectively.

Table S6: Computed energy levels (the ground state is set at zero), composition of the g-tensor and contributions to the wave function for each M_J state of the ground-state multiplet for the model 4. KD stands for Kramers doublet.

KD	E (cm $^{-1}$)	g_x	g_y	g_z	wave function composition*
1	0	0.000	0.000	19.821	$99.6 \pm 15/2>$
2	484.2	1.715	6.776	13.243	$37.1 \pm 13/2> + 19.2 \pm 1/2> + 15.2 \pm 5/2> + 13.2 \pm 3/2>$
3	571.1	3.411	3.953	7.914	$53.1 \pm 13/2> + 17.4 \pm 3/2> + 14.5 \pm 1/2>$
4	847.8	7.595	7.253	4.573	$43.7 \pm 11/2> + 15.5 \pm 5/2> + 15.4 \pm 7/2>$
5	1166.5	0.839	1.396	11.551	$36.4 \pm 11/2> + 29.9 \pm 9/2> + 15.9 \pm 3/2>$
6	1600	0.377	0.555	14.430	$36.7 \pm 9/2> + 30.0 \pm 7/2> + 14.4 \pm 1/2> + 11.8 \pm 11/2>$
7	2046.8	0.079	0.117	16.955	$33.3 \pm 5/2> + 31.2 \pm 7/2> + 17.2 \pm 3/2> + 14.3 \pm 9/2>$
8	2277.1	0.030	0.035	19.625	$38.6 \pm 1/2> + 32.1 \pm 3/2> + 20.0 \pm 5/2>$

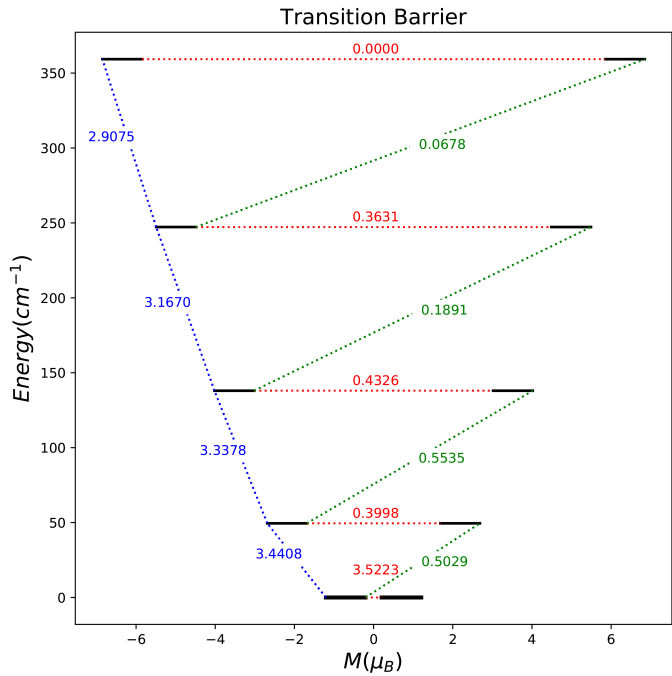


Figure S9: Computed magnetization blocking barriers for **5**. The four lowest Kramers doublets (thick black lines) are represented according to their magnetic moment along the main magnetic axis. The blue lines represent vertical excitations, the green dashed lines correspond to possible Orbach relaxation processes while the red lines correspond to QTM/TA-QTM processes. The values correspond to the mean value of the corresponding transversal matrix element of the transition magnetic moment.

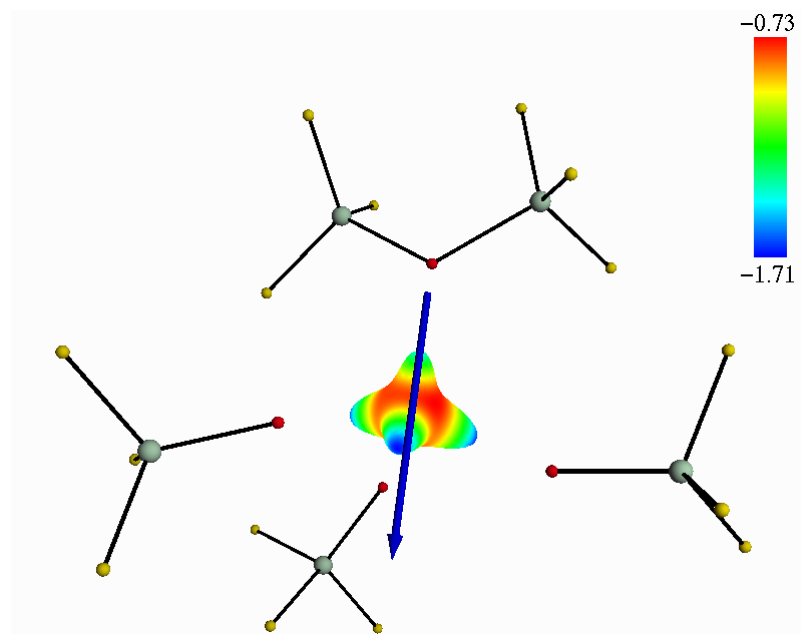


Figure S10: Representation of the total electrostatic potential (expressed in $e^- \cdot \text{bohr}^{-1}$) at 2.5 Å around the Dy(III) ion with g_z direction in blue line for **5**. The lowest and highest values are in blue and red, respectively.

Table S7: Computed energy levels (the ground state is set at zero), composition of the g-tensor and contributions to the wave function for each M_J state of the ground-state multiplet for the model **5**. KD stands for Kramers doublet.

KD	E (cm ⁻¹)	g_x	g_y	g_z	wave function composition*
1	0	11.662	9.472	1.409	$94.4 \pm 1/2\rangle$
2	49.5	0.166	1.999	4.394	$94.8 \pm 3/2\rangle$
3	138	0.221	2.087	7.050	$89.6 \pm 5/2\rangle$
4	247.2	0.850	1.313	9.998	$84.4 \pm 7/2\rangle + 10.2 \pm 13/2\rangle$
5	359.3	0.186	0.264	12.750	$79.8 \pm 9/2\rangle + 10.9 \pm 15/2\rangle$
6	458.2	0.075	0.120	15.005	$77.4 \pm 11/2\rangle + 11.8 \pm 13/2\rangle$
7	515.6	0.071	0.150	16.946	$63.7 \pm 13/2\rangle + 18.6 \pm 15/2\rangle$
8	568.4	0.024	0.032	19.026	$66.5 \pm 15/2\rangle + 13.3 \pm 9/2\rangle + 11.9 \pm 13/2\rangle$

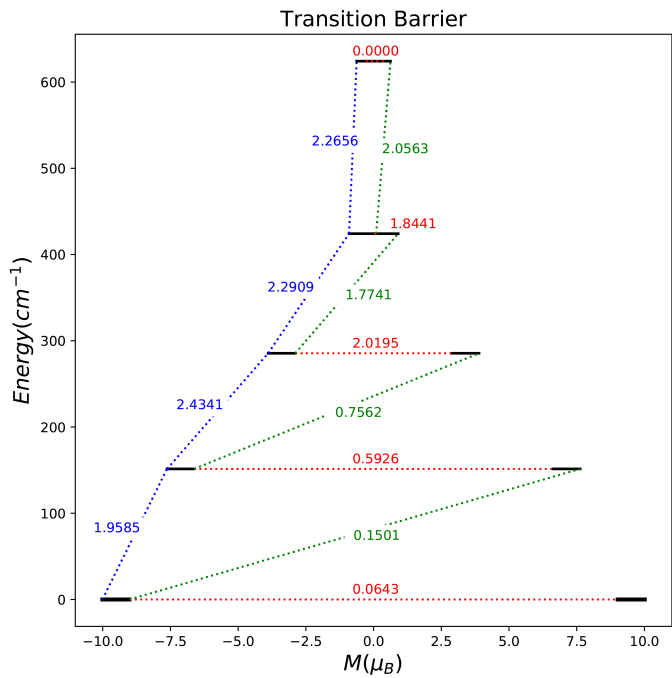


Figure S11: Computed magnetization blocking barriers for **6**. The four lowest Kramers doublets (thick black lines) are represented according to their magnetic moment along the main magnetic axis. The blue lines represent vertical excitations, the green dashed lines correspond to possible Orbach relaxation processes while the red lines correspond to QTM/TA-QTM processes. The values correspond to the mean value of the corresponding transversal matrix element of the transition magnetic moment.

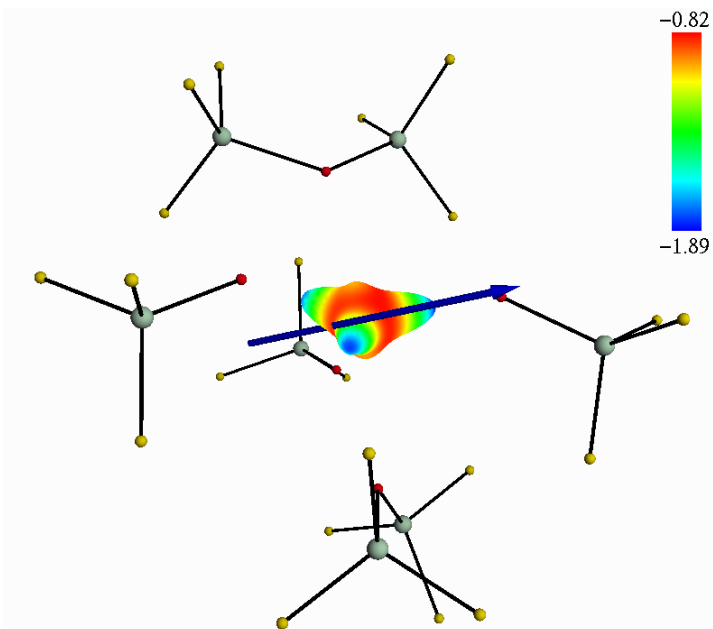


Figure S12: Representation of the total electrostatic potential (expressed in $e^- \cdot \text{bohr}^{-1}$) at 2.5 Å around the Dy(III) ion with g_z direction in blue line for **6**. The lowest and highest values are in blue and red, respectively.

Table S8: Computed energy levels (the ground state is set at zero), composition of the g-tensor and contributions to the wave function for each M_J state of the ground-state multiplet for the model **6**. KD stands for Kramers doublet.

KD	E (cm^{-1})	g_x	g_y	g_z	wave function composition*
1	0	0.113	0.273	19.024	$87.0 \pm 15/2\rangle + 11/2\rangle$
2	151.4	1.220	2.299	14.436	$64.1 \pm 13/2\rangle + 23.8 \pm 9/2\rangle$
3	285.5	7.568	6.719	4.526	$28.0 \pm 7/2\rangle + 23.6 \pm 11/2\rangle + 18.3 \pm 3/2\rangle + 10.4 \pm 1/2\rangle$
4	424.2	0.654	1.183	9.418	$24.8 \pm 5/2\rangle + 23.8 \pm 11/2\rangle + 16.9 \pm 1/2\rangle + 14.8 \pm 13/2\rangle$
5	624.2	0.167	0.233	12.227	$24.9 \pm 9/2\rangle + 23.3 \pm 3/2\rangle + 22.8 \pm 11/2\rangle$
6	867.1	0.047	0.054	14.842	$26.3 \pm 9/2\rangle + 25.8 \pm 7/2\rangle + 20.1 \pm 1/2\rangle + 13.1 \pm 11/2\rangle$
7	1072.9	0.002	0.002	18.077	$28.8 \pm 5/2\rangle + 22.8 \pm 7/2\rangle + 21.9 \pm 3/2\rangle + 11.5 \pm 9/2\rangle + 10.4 \pm 1/2\rangle$
8	1180.7	0.000	0.001	19.793	$33.3 \pm 1/2\rangle + 28.7 \pm 3/2\rangle + 20.4 \pm 5/2\rangle + 11.3 \pm 7/2\rangle$

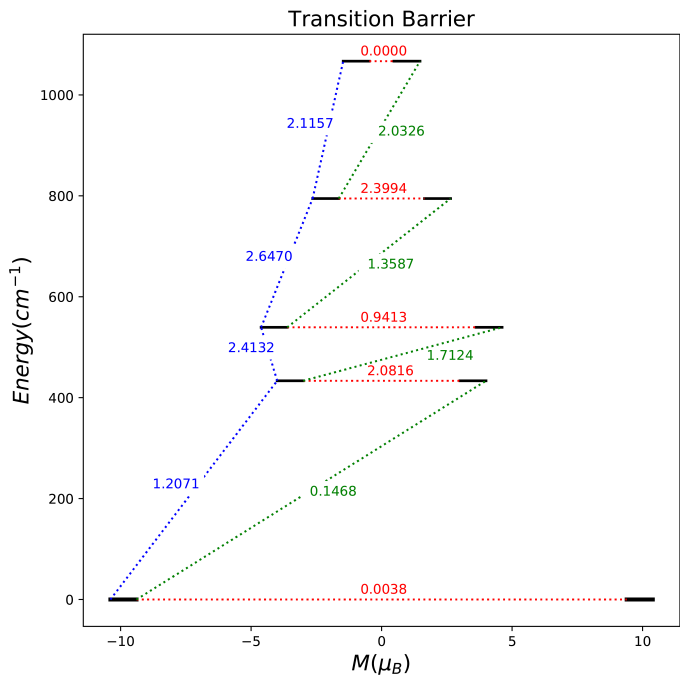


Figure S13: Computed magnetization blocking barriers for **7**. The four lowest Kramers doublets (thick black lines) are represented according to their magnetic moment along the main magnetic axis. The blue lines represent vertical excitations, the green dashed lines correspond to possible Orbach relaxation processes while the red lines correspond to QTM/TA-QTM processes. The values correspond to the mean value of the corresponding transversal matrix element of the transition magnetic moment.

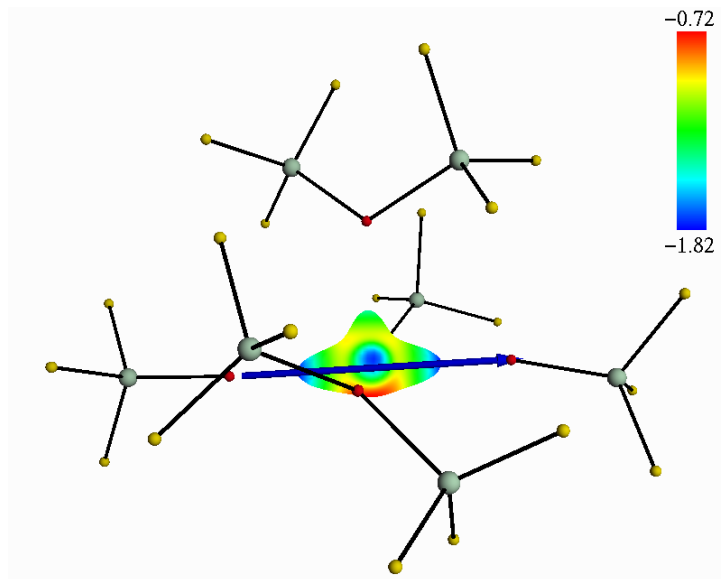


Figure S14: Representation of the total electrostatic potential (expressed in $e^- \cdot \text{bohr}^{-1}$) at 2.5 Å around the Dy(III) ion with g_z direction in blue line for **7**. The lowest and highest values are in blue and red, respectively.

Table S9: Computed energy levels (the ground state is set at zero), composition of the g-tensor and contributions to the wave function for each M_J state of the ground-state multiplet for the model **7**. KD stands for Kramers doublet.

KD	E (cm $^{-1}$)	g_x	g_y	g_z	wave function composition*
1	0	0.008	0.015	19.783	$99.3 \pm 15/2>$
2	433.5	1.670	5.137	14.726	$31.8 \pm 13/2> + 21.2 \pm 1/2> + 16.4 \pm 5/2> + 14.7 \pm 3/2>$
3	539.4	1.393	4.104	9.071	$57.2 \pm 13/2> + 16.9 \pm 3/2> + 13.3 \pm 1/2>$
4	794.6	7.667	7.254	3.988	$41.7 \pm 11/2> + 14.7 \pm 5/2> + 13.6 \pm 7/2> + 10.6 \pm 1/2>$
5	1066.9	0.985	2.032	11.350	$38.1 \pm 11/2> + 28.2 \pm 9/2> + 15.4 \pm 3/2>$
6	1371.1	0.509	0.938	14.240	$38.4 \pm 9/2> + 30.6 \pm 7/2> + 12.3 \pm 1/2> + 11.5 \pm 11/2>$
7	1621.5	0.080	0.363	17.502	$31.2 \pm 5/2> + 28.0 \pm 7/2> + 17.4 \pm 3/2> + 13.5 \pm 9/2>$
8	1696.1	0.149	0.152	19.547	$31.4 \pm 1/2> + 30.4 \pm 3/2> + 22.2 \pm 5/2> + 12.6 \pm 7/2>$

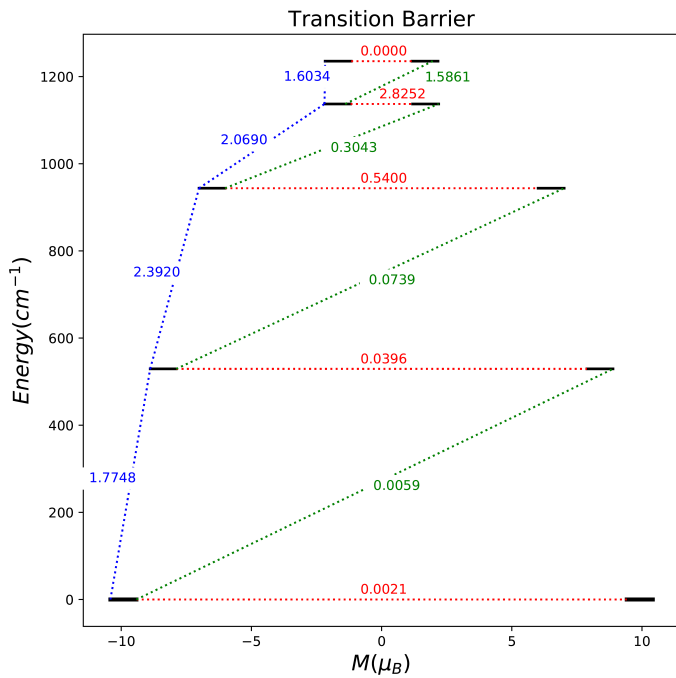


Figure S15: Computed magnetization blocking barriers for **8**. The four lowest Kramers doublets (thick black lines) are represented according to their magnetic moment along the main magnetic axis. The blue lines represent vertical excitations, the green dashed lines correspond to possible Orbach relaxation processes while the red lines correspond to QTM/TA-QTM processes. The values correspond to the mean value of the corresponding transversal matrix element of the transition magnetic moment.

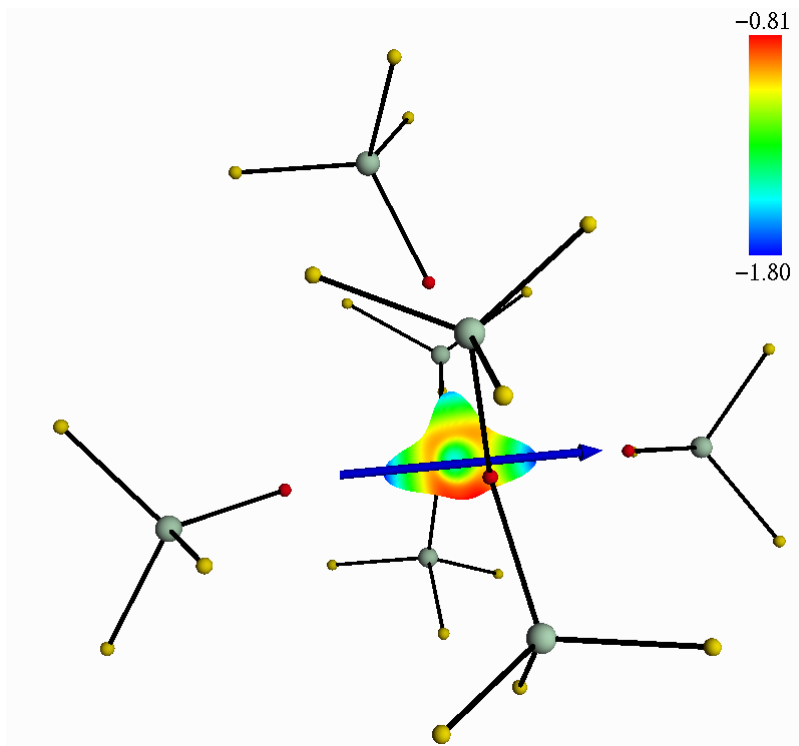


Figure S16: Representation of the total electrostatic potential (expressed in $e^- \cdot \text{bohr}^{-1}$) at 2.5 Å around the Dy(III) ion with g_z direction in blue line for **8**. The lowest and highest values are in blue and red, respectively.

Table S10: Computed energy levels (the ground state is set at zero), composition of the g-tensor and contributions to the wave function for each M_J state of the ground-state multiplet for the model **8**. KD stands for Kramers doublet.

KD	E (cm ⁻¹)	g_x	g_y	g_z	wave function composition*
1	0	0.005	0.007	19.830	$99.7 \pm 15/2>$
2	529.2	0.106	0.131	16.818	$98.0 \pm 13/2>$
3	943.8	1.578	1.628	13.299	$86.2 \pm 11/2>$
4	1137.2	2.926	3.633	15.211	$52.7 \pm 1/2> + 20.5 \pm 9/2>$
5	1235.3	0.487	2.847	11.055	$38.7 \pm 9/2> + 34.6 \pm 3/2> + 10.0 \pm 7/2>$
6	1320.6	0.568	4.518	13.815	$40.1 \pm 5/2> + 32.2 \pm 7/2> + 10.0 \pm 3/2>$
7	1469.7	0.330	2.111	15.034	$27.5 \pm 1/2> + 24.6 \pm 3/2> + 23.9 \pm 9/2> + 13.5 \pm 7/2>$
8	1557.5	0.783	2.859	16.550	$35.1 \pm 7/2> + 34.4 \pm 5/2> + 15.5 \pm 3/2>$

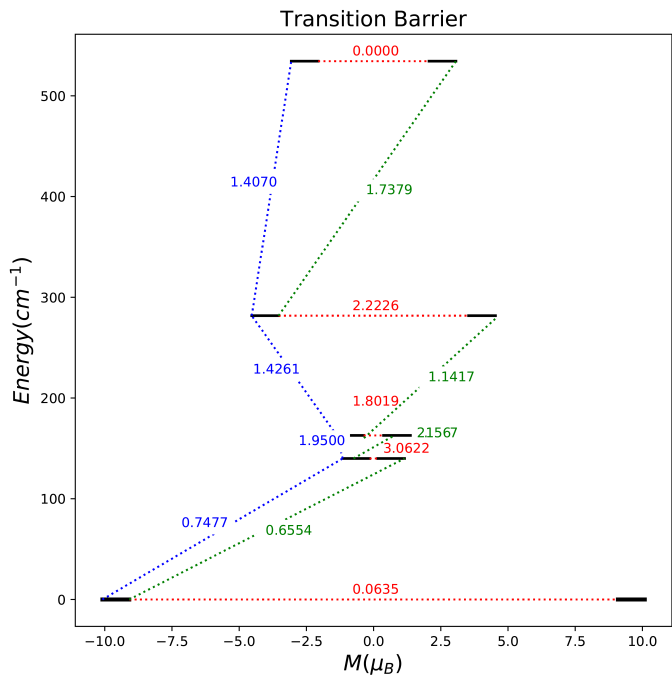


Figure S17: Computed magnetization blocking barriers for **9**. The four lowest Kramers doublets (thick black lines) are represented according to their magnetic moment along the main magnetic axis. The blue lines represent vertical excitations, the green dashed lines correspond to possible Orbach relaxation processes while the red lines correspond to QTM/TA-QTM processes. The values correspond to the mean value of the corresponding transversal matrix element of the transition magnetic moment.

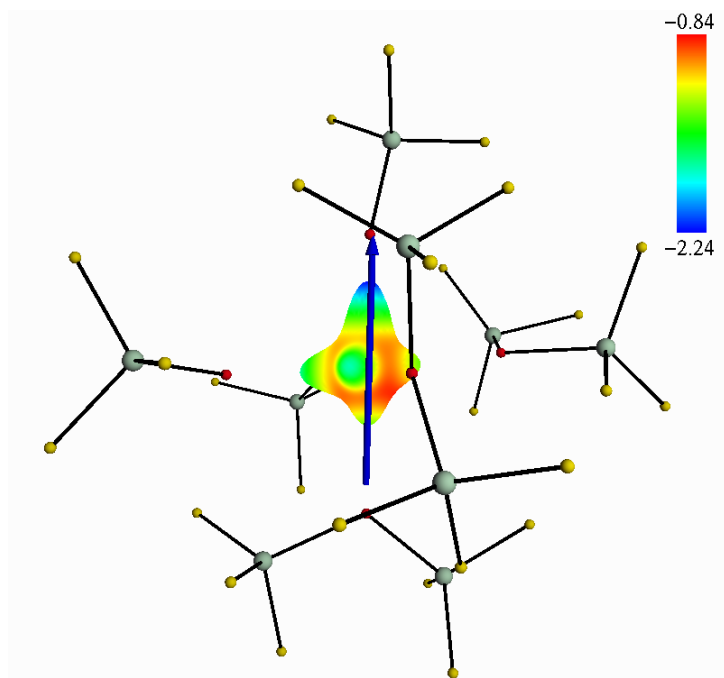


Figure S18: Representation of the total electrostatic potential (expressed in $e^- \cdot \text{bohr}^{-1}$) at 2.5 Å around the Dy(III) ion with g_z direction in blue line for **9**. The lowest and highest values are in blue and red, respectively.

Table S11: Computed energy levels (the ground state is set at zero), composition of the g-tensor and contributions to the wave function for each M_J state of the ground-state multiplet for the model **9**. KD stands for Kramers doublet.

KD	E (cm $^{-1}$)	g_x	g_y	g_z	wave function composition*
1	0	0.031	0.350	19.176	$94.9 \pm 15/2>$
2	140	11.544	8.718	1.072	$83.3 \pm 1/2>$
3	162.9	10.227	7.621	0.298	$52.5 \pm 3/2> + 24.6 \pm 5/2> + 13.0 \pm 13/2>$
4	281.8	8.112	7.271	6.029	$52.7 \pm 13/2> + 25.2 \pm 3/2> + 12.6 \pm 5/2>$
5	534.4	7.059	5.055	1.040	$47.3 \pm 5/2> + 27.4 \pm 13/2> + 16.0 \pm 11/2>$
6	590.6	8.847	7.288	0.657	$57.1 \pm 7/2> + 21.7 \pm 9/2>$
7	641.2	9.253	6.804	1.094	$55.1 \pm 11/2> + 15.2 \pm 3/2> + 15.2 \pm 7/2>$
8	705.6	1.793	3.142	14.604	$64.4 \pm 9/2> + 13.2 \pm 7/2> + 11.4 \pm 11/2>$

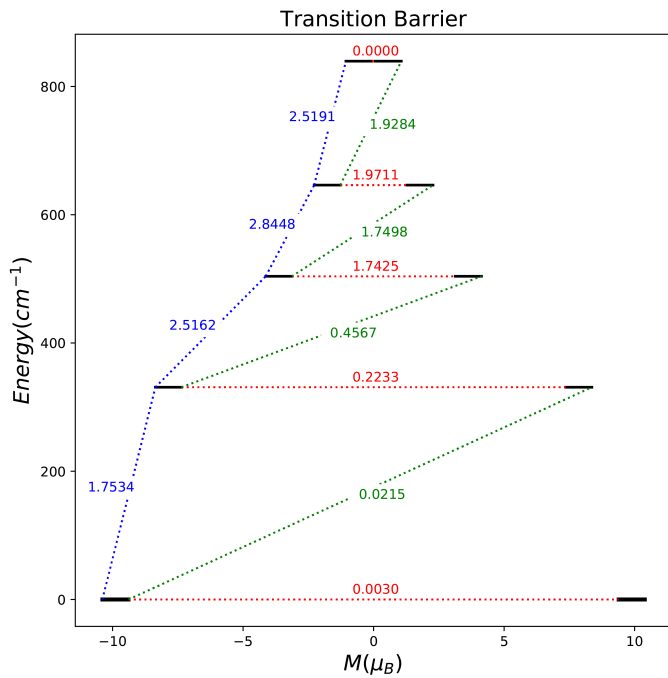


Figure S19: Computed magnetization blocking barriers for **10**. The four lowest Kramers doublets (thick black lines) are represented according to their magnetic moment along the main magnetic axis. The blue lines represent vertical excitations, the green dashed lines correspond to possible Orbach relaxation processes while the red lines correspond to QTM/TA-QTM processes. The values correspond to the mean value of the corresponding transversal matrix element of the transition magnetic moment.

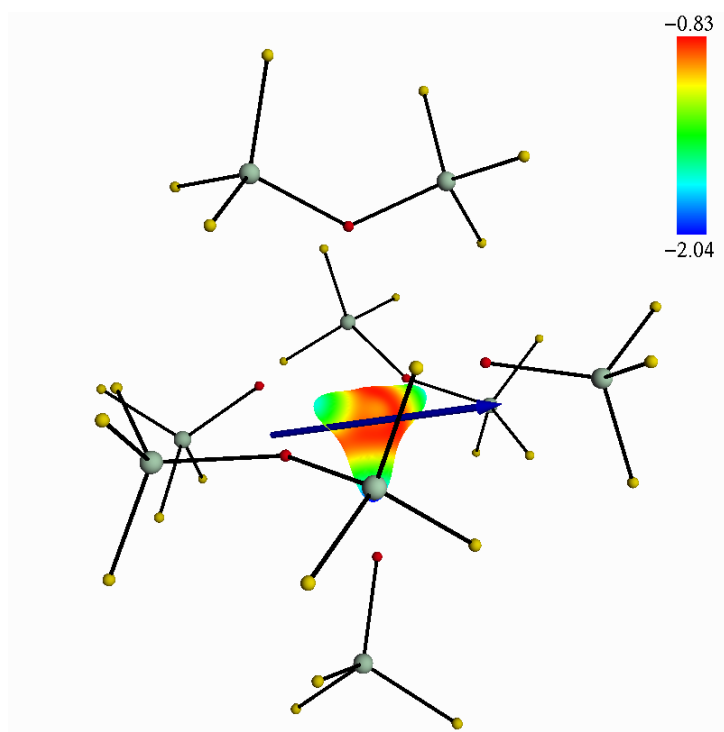


Figure S20: Representation of the total electrostatic potential (expressed in $e^- \cdot \text{bohr}^{-1}$) at 2.5 Å around the Dy(III) ion with g_z direction in blue line for **10**. The lowest and highest values are in blue and red, respectively.

Table S12: Computed energy levels (the ground state is set at zero), composition of the g-tensor and contributions to the wave function for each M_J state of the ground-state multiplet for the model **10**. KD stands for Kramers doublet.

KD	E (cm $^{-1}$)	g_x	g_y	g_z	wave function composition*
1	0	0.007	0.011	19.780	$98.6 \pm 15/2>$
2	331	0.434	0.886	16.080	$82.9 \pm 13/2>$
3	504	3.184	4.519	11.689	$28.8 \pm 11/2> + 19.5 \pm 3/2> + 19.1 \pm 7/2> + 13.9 \pm 1/2>$
4	646.2	2.945	4.546	7.978	$38.2 \pm 11/2> + 19.4 \pm 5/2> + 18.4 \pm 1/2> + 12.8 \pm 9/2>$
5	839.5	0.821	1.254	11.612	$34.2 \pm 9/2> + 21.3 \pm 3/2> + 19.3 \pm 11/2>$
6	1066.3	0.173	0.243	14.518	$30.8 \pm 7/2> + 27.6 \pm 9/2> + 16.9 \pm 1/2> + 11.1 \pm 5/2>$
7	1259.3	0.024	0.044	17.715	$27.9 \pm 5/2> + 23.5 \pm 3/2> + 21.3 \pm 7/2> + 16.0 \pm 1/2>$
8	1345	0.008	0.012	19.737	$28.3 \pm 1/2> + 27.8 \pm 3/2> + 23.5 \pm 5/2> + 14.5 \pm 7/2>$

1				2			
Y	-0.006463	0.009208	-0.000037	Y	-0.00099	0.354378	-0.96939
O	1.588596	1.324173	0.000011	Si	-3.2121	1.422897	0.270973
O	-1.934395	0.750302	-0.000018	Si	3.20832	1.428886	0.270955
O	0.321246	-2.031413	-0.000037	Si	0.004394	-3.08965	0.155776
Si	2.830483	2.347983	0.000048	F	-4.37707	0.956563	-0.71053
F	4.222517	1.576493	0.000029	F	-3.51566	2.926596	0.691208
F	2.804181	3.285852	1.285842	F	-3.30178	0.526104	1.584056
F	2.804187	3.285919	-1.285698	F	4.371863	0.959401	-0.71078
Si	-3.461898	1.257204	0.000017	F	3.299935	0.536294	1.586734
F	-3.554505	2.845937	-0.000371	F	3.512488	2.93394	0.685859
F	-4.240044	0.734356	1.286717	F	-1.27491	-3.95835	-0.21862
F	-4.240308	0.733722	-1.286266	F	0.001416	-2.87418	1.732717
Si	0.635258	-3.61023	-0.000032	F	1.290248	-3.95032	-0.21481
F	-0.700761	-4.474671	-0.000079	O	-1.77059	1.272936	-0.4304
F	1.474259	-4.028979	1.286389	O	1.765899	1.276709	-0.42806
F	1.474329	-4.028963	-1.286412	O	0.001123	-1.67404	-0.61582

3			
Y	-0.40698	-0.97158	-0.05155
O	-2.53731	-0.76453	-0.01383
O	1.722194	-1.17756	-0.0892
O	-0.20008	1.166573	-0.04843
Si	3.326889	-1.16254	0.019306
F	3.958356	-2.41465	-0.74196
F	3.808266	-1.25288	1.535316
F	3.962052	0.143056	-0.62903
Si	-4.07684	-0.31054	0.019546
F	-5.05353	-1.57211	0.018386
F	-4.46037	0.573683	-1.24807
F	-4.41551	0.536593	1.324857
Si	1.029667	2.206218	-0.00718
F	2.100111	1.785116	1.104644
F	0.546216	3.678606	0.351905
F	1.785269	2.281661	-1.40733

4				5			
Y	0.009941	0.335517	-0.054697	Y	0.001528	0.346146	0.043319
Si	2.620898	2.749638	0.071728	O	-1.06613	-1.48632	-0.26184
Si	-3.087051	2.388324	-0.322937	O	-1.37156	1.962854	0.346628
Si	3.298909	-1.371973	0.166286	O	1.230399	0.760535	-1.66188
F	3.445127	2.844138	-1.290498	Si	-2.7774	-1.54046	-0.27851
F	2.598474	4.214561	0.702392	F	-3.13959	-3.04202	-0.60179
F	3.481557	1.847634	1.080724	F	-3.23564	-0.56483	-1.42017
F	-2.797084	3.81981	0.309191	F	-3.25521	-1.11635	1.154746
F	-3.708706	2.618868	-1.77267	Si	-2.79084	2.675759	0.51703
F	-4.239725	1.720162	0.569229	F	-2.98076	3.366824	1.938534
F	4.266092	-0.484576	-0.735335	F	-3.96635	1.586045	0.382546
F	3.972135	-1.556612	1.597078	F	-3.0745	3.781372	-0.59284
F	3.259619	-2.824744	-0.510169	Si	2.677702	1.370248	-1.98943
O	1.151613	2.152954	-0.142948	F	3.696445	0.264445	-2.51795
O	1.816858	-0.770121	0.244949	F	3.317228	2.032338	-0.67952
O	-1.797614	1.44248	-0.354671	F	2.616045	2.509866	-3.10158
O	-1.134786	-1.486713	0.033781	O	1.249516	0.149935	1.773205
Si	-2.644114	-1.441962	0.814597	Si	2.771492	-0.16743	2.165177
F	-2.874033	-2.879556	1.422739	F	2.867779	-1.38915	3.188979
F	-3.78872	-1.080785	-0.193228	F	3.521946	1.064914	2.833852
F	-2.397376	-0.385476	1.965455	F	3.609402	-0.60607	0.87211
Si	-0.449769	-2.865534	-0.688097	Si	-0.14234	-2.90176	-0.50284
F	0.334897	-2.240144	-1.911964	F	1.324927	-2.3417	-0.35488
F	-1.653683	-3.749291	-1.195941	F	-0.43082	-3.45999	-1.94171
F	0.432483	-3.665418	0.32991	F	-0.50848	-3.94178	0.615409

6				7			
Y	0.006681	-0.008716	0.357694	Y	0.02562	0.079922	-0.82293
O	-2.269839	0.301502	-0.702432	Si	-0.62725	3.216222	-0.65135
O	2.468661	-0.340896	0.755843	Si	1.82463	2.487275	0.831067
Si	3.457289	0.973238	0.415922	Si	-3.63619	0.674078	-0.64027
Si	2.883928	-1.933732	1.008092	Si	3.679888	-0.51192	-1.33228
Si	-3.251192	1.395246	0.077721	Si	-1.22724	-3.16581	-1.25687
Si	-2.660153	-0.821223	-1.885023	F	-1.87139	3.459031	0.268778
O	0.143278	-0.763426	-1.614902	F	0.203373	4.547583	-0.81883
O	0.799402	1.930688	0.576419	F	-0.95083	2.595357	-2.07827
O	-0.798032	-1.067347	1.982972	F	2.192974	1.256467	1.741314
F	-2.252682	-2.265247	-1.395427	F	2.956417	2.899964	-0.17516
F	-2.073258	-0.44779	-3.301358	F	1.402766	3.721165	1.723691
F	-4.241901	-0.730493	-1.989122	F	-3.86425	2.10336	-1.33154
F	-2.322034	1.83209	1.296267	F	-4.34819	0.742719	0.787728
F	-4.589967	0.760073	0.604737	F	-4.42552	-0.39122	-1.51715
F	-3.581825	2.611407	-0.866202	F	4.575953	0.550566	-0.53484
F	1.547285	-2.699175	0.613254	F	4.131586	-0.43496	-2.85895
F	3.127307	1.534341	-1.021485	F	4.098825	-1.94763	-0.7766
F	4.921077	0.359038	0.40429	F	-1.20803	-3.37992	0.352756
F	3.41207	2.062105	1.555903	F	-0.67109	-4.52168	-1.88291
Si	0.511227	3.496714	0.389364	F	-2.76962	-3.07739	-1.65278
F	1.713518	4.24398	-0.338401	O	0.4285	2.041747	-0.02836
F	0.240189	4.253532	1.762683	O	2.123781	-0.2104	-1.13505
F	-0.798421	3.690937	-0.51751	O	-2.0707	0.370562	-0.51189
Si	1.187757	-1.188614	-2.751358	O	-0.37491	-1.8749	-1.61688
F	0.761791	-2.516833	-3.515227	O	0.085518	-0.85137	1.170758
F	2.619445	-1.474752	-2.069194	Si	-1.12308	-0.42125	2.283418
F	1.427707	-0.057943	-3.84387	F	-0.54069	-0.74563	3.717856
Si	-2.061432	-1.911168	2.483087	F	-2.46832	-1.19412	2.05512
F	-2.516766	-1.546427	3.963516	F	-1.26529	1.154151	2.175203
F	-1.827115	-3.484829	2.429854	Si	1.165519	-2.13298	1.539473
F	-3.316339	-1.5952	1.524395	F	2.453251	-1.46389	2.159667
F	3.20393	-2.160706	2.536316	F	1.550339	-2.96057	0.264321
F	4.106852	-2.400411	0.137415	F	0.448342	-3.02008	2.629547

8			
Y	-0.03831	0.371465	-0.14898
Si	0.522776	-2.91854	1.570293
Si	2.850949	0.15482	1.602221
Si	-2.7207	1.920525	1.719503
Si	2.362215	-0.87183	-2.43554
Si	-2.80134	-1.61434	-0.14654
Si	-2.47248	0.505276	-2.21482
F	1.053349	-3.87739	0.411724
F	1.607474	-2.97936	2.744433
F	-0.81633	-3.5867	2.134293
F	3.251526	-1.21605	0.949659
F	4.128746	1.089937	1.738401
F	2.151568	0.026689	3.002528
F	-3.05428	1.528224	3.225719
F	-2.96785	3.492258	1.584863
F	-3.85901	1.227806	0.803142
F	3.455686	0.075092	-1.70563
F	2.949299	-2.34945	-2.38587
F	2.372538	-0.42018	-3.96726
F	-2.05693	-2.956	-0.49743
F	-4.20684	-1.58216	-0.87733
F	-2.93191	-1.39173	1.400957
F	-1.29383	1.589086	-2.27167
F	-3.8604	1.213555	-2.03787
F	-2.47528	-0.41399	-3.48931
O	0.268969	-1.41694	1.096494
O	1.862071	1.074626	0.56138
O	0.952135	-0.6805	-1.72574
O	-1.28484	1.460799	1.213424
O	-1.94692	-0.33046	-0.86186
Si	2.262823	2.608946	0.014959
F	3.625274	2.712266	-0.75165
F	2.200111	3.6531	1.188651
F	1.018592	2.794398	-0.97817

9				10			
Y	0.007804	0.002708	0.324527	Y	-0.01109	-0.4302	0.312008
O	1.703719	-0.484562	1.566093	O	0.37053	1.376812	1.388696
O	-1.190943	-1.220249	1.446083	O	0.967784	1.833561	-1.31142
O	-1.807378	0.54279	-0.854579	O	0.348487	-1.35174	-1.59825
O	1.408907	1.28488	-0.815679	O	-0.98869	-1.86843	1.436934
O	-0.431605	1.680225	1.616438	Si	0.246956	2.307946	-2.71053
O	0.410651	-1.86695	-0.817059	F	0.808548	3.724781	-3.13539
Si	-3.259581	-0.063698	-0.161603	F	-1.3104	2.442105	-2.41948
F	-4.363367	0.680731	-1.03225	F	0.482133	1.259667	-3.86361
F	-3.502969	0.291441	1.345948	Si	2.208701	2.528458	-0.46943
F	-3.325369	-1.607867	-0.493869	F	1.734757	3.731026	0.438369
Si	-1.972692	1.537949	-2.21001	F	3.242396	3.102583	-1.52637
F	-0.491948	1.679267	-2.770905	F	2.970007	1.399075	0.351743
F	-2.527422	2.955932	-1.825618	Si	0.568698	1.99085	2.861255
F	-2.867826	0.847528	-3.3068	F	0.244755	0.923649	4.001859
Si	2.35222	0.924317	-2.171946	F	-0.37211	3.252202	3.117706
F	2.213642	2.046722	-3.268515	F	2.078301	2.458889	3.087005
F	1.724511	-0.422658	-2.736575	Si	-2.36511	-2.4233	2.044082
F	3.855112	0.684574	-1.784462	F	-2.37177	-2.45792	3.634173
Si	1.624611	2.848467	-0.128269	F	-2.71959	-3.88739	1.53481
F	0.312596	3.665634	-0.459068	F	-3.5801	-1.46735	1.595691
F	2.816291	3.42794	-1.007452	Si	-0.43691	-2.56364	-2.30272
F	2.060165	2.886853	1.376119	F	-0.51257	-2.44016	-3.88653
Si	3.146818	-0.116447	2.130688	F	-1.94952	-2.5929	-1.74514
F	3.909945	0.870898	1.106582	F	0.175401	-3.99342	-1.96333
F	4.089234	-1.398767	2.277492	O	2.349602	-1.39008	0.297117
F	3.133486	0.61559	3.543292	O	-2.31065	0.579985	-0.20398
Si	-1.674259	-2.543307	2.205242	Si	3.047515	-1.57156	1.797078
F	-1.285194	-3.841182	1.341868	F	3.402233	-3.08706	2.050606
F	-3.261622	-2.581033	2.374244	F	1.891197	-1.0902	2.772574
F	-1.035948	-2.725873	3.649048	F	4.329355	-0.67448	1.971108
Si	-0.368977	-2.530531	-2.15964	Si	3.089469	-1.57131	-1.19498
F	0.669876	-2.986584	-3.252637	F	2.936911	-0.25713	-2.06284
F	-1.233943	-1.338452	-2.756439	F	2.682217	-2.88059	-1.97235
F	-1.315177	-3.709515	-1.730203	F	4.626146	-1.72525	-0.80993
Si	1.650714	-2.823469	-0.103669	Si	-3.24433	0.242197	-1.55892
F	1.556268	-4.153719	-0.973743	F	-4.2312	-0.95174	-1.29107
Si	-1.489692	2.755568	2.125074	F	-2.24462	-0.0892	-2.73922
F	-2.696717	2.899641	1.060828	F	-4.0702	1.548085	-1.89506
F	-0.861377	4.21877	2.261137	Si	-2.88601	1.564847	1.029484
F	-2.161622	2.406483	3.525127	F	-2.35148	1.003377	2.406811
F	1.428964	-3.22651	1.395436	F	-4.4646	1.515908	0.98035
F	3.029365	-2.123462	-0.430706	F	-2.3895	3.041705	0.792442

References

- [1] M. F. Delley, G. Lapadula, F. Núñez-Zarur, A. Comas-Vives, V. Kalendra, G. Jeschke, D. Baabe, M. D. Walter, A. J. Rossini, A. Lesage, L. Emsley, O. Maury, C. Copéret, *Journal of the American Chemical Society* **2017**, *139*, 8855–8867.